Low & High & Multiple Energy Scales @ HERA

Günter Grindhammer (for the H1 and ZEUS collaborations)
Max-Planck-Institut für Physik , Föhringer Ring 6, 80805 Munich, Germany

DOI: will be assigned

The latest QCD results from the H1 and ZEUS collaborations at HERA presented here cover a wide range in the energy scales relevant for the strong interactions. They comprise a study of the underlying event, measurements of jet production and of $\alpha_s(M_Z)$ as well as measurements of heavy flavor cross sections including the charm and beauty structure functions.

1 Introduction

Recent results from HERA on the hadronic final state in deep-inelastic scattering (DIS) and photoproduction (PHP) are presented, covering a wide range in the energy scales relevant for the strong interactions. The study of the underlying event probes low and high scales, while jet production is dominated by high scales. In heavy flavor production multiple scales play a role.

The HERA *ep*-collider operated with electrons or positrons of 27.6 GeV and protons of 820 or 920 GeV. Each of the two collider experiments H1 and ZEUS collected about 120 pb^{-1} from 1995 to 2000 (HERA-1) and after a luminosity upgrade about 370 pb^{-1} from 2003 to 2007 (HERA-2). Since the results presented here do not depend on whether the incident lepton was an electron or a positron, the term "electron" is used to mean either of them. During part of HERA-1 only H1 and since HERA-2 both experiments were equipped with micro-vertex detectors, which is of particular relevance for some of the heavy flavor results shown. The DIS kinematic region is defined by measuring the scattered electron in the main detector with photon virtualities $Q^2 > 1\,\text{GeV}^2$. The PHP region is defined by either not observing a scattered electron ($Q^2 < 1\,\text{GeV}^2$) or by requiring a signal in designated electron taggers ($Q^2 < 0.01\,\text{GeV}^2$). Requirements on the inelasticity y, measured via the scattered electron or the hadronic final state, complete the definition of the DIS or PHP phase space.

The slides of the talk which include more figures than possible in this written version can be found in [1].

2 Low & high scales: Underlying event in PHP

In *ep* collisions the quasi-real photon can directly interact with a parton from the proton or it can have fluctuated into partons of which one interacts with a parton from the proton as exemplified in Fig. 1. In the latter case additional interactions between the remnant partons of the photon and the proton may occur. They are usually referred to as underlying event and/or multi-parton interactions (MPI).

In leading order (LO) QCD one can distinguish between these *direct* and *resolved* interactions by measuring the transverse energies and pseudo-rapidities of the two hard jets and constructing the observable $x_\gamma = 1/(2yE_e)\,(E_{\mathrm{T,jet1}}\exp^{-\eta_{\mathrm{jet1}}} + E_{\mathrm{T,jet2}}\exp^{-\eta_{\mathrm{jet2}}})$, i.e. the fractional photon energy carried by the parton from the photon. For direct events $x_\gamma \to 1$ and for resolved events $0 < x_\gamma < 1$. Thus, at HERA MPI can be turned *on* by studying events with typically $x_\gamma < 0.7$ or *off* for $x_\gamma > 0.7$.

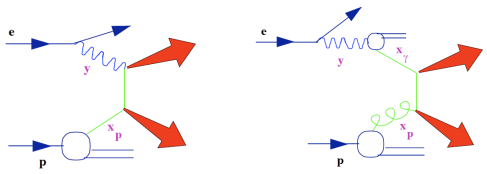

Figure 1: A direct (left) and a resolved (right) photon interaction diagram.

In case of a resolved photon event the additional interactions, besides the primary hard parton-parton interaction leading to a hard dijet, are of interest. The MPI may consist of additional *soft* interactions affecting the particle multiplicity, but also of *semi-hard* interactions leading to an increase in jet multiplicity. The interpretation of the measurements in terms of MPI is unfortunately not straightforward. Other effects, more or less well understood, due to additional parton radiation (higher order QCD effects), fragmentation and beam remnants, may lead to similar signatures as MPI. Since MPI provide an important background to precise QCD measurements and to searches for new physics, particularly at the TEVATRON and soon at the LHC, it is of great interest to improve the understanding and modeling of them.

H1 provided new preliminary measurements [2] of the mean charged particle multiplicity in different azimuthal regions. The method, illustrated in Fig. 2, follows closely an analysis [3] by the CDF collaboration. In PHP events, $Q^2 < 0.01\,\mathrm{GeV}^2$ and $0.3 < y < 0.65$, a leading and a sub-leading jet with $P_{\mathrm{T,jet}} > 5$ GeV and $|\eta_{\mathrm{jet}}| < 1.5$ were required. The jets were reconstructed in the laboratory frame using the longitudinally invariant $k_\perp$-cluster algorithm [4]. The leading jet at $\Phi^\star = 0^\circ$ defines the *Toward region*, and the sub-leading jet is usually found in the *Away region*. The mean charged particle multiplicity, using tracks with $P_{\mathrm{T}} > 150$ MeV and $|\eta| < 1.5$, was measured in these and the transverse regions. The transverse regions are distinguished into *High* and *Low activity regions* depending on in which region the scalar sum over the transverse particle momenta is higher. The expectation is that the transverse regions, particularly the *Low activity region*, shows sensitivity to MPI.

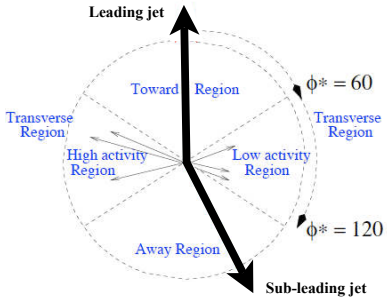

Figure 2: Definition of the four azimuthal regions.

For events satisfying the above mentioned requirements, the dependence of the mean charged particle multiplicity on the angle $\Delta\Phi$ between the leading jet and the charged particles is shown in [1, 2] together with comparisons to Pythia [5] simulations. It is observed that the resolved-enhanced events ($x_\gamma < 0.7$) are described by Pythia only when MPI are included.

The Pythia event generation includes direct and resolved processes in LO matched with DGLAP-type parton showers. MPI are simulated with additional *semi-hard* interactions down to $P_{\mathrm{T}} = 1.2$ GeV. The data are also compared to Cascade [6, 7] which contains direct processes using off-shell matrix elements in LO matched with CCFM-type parton showers, where the gluon emissions are not ordered in k_{T}. The gluon in the proton is described by k_{T} un-integrated gluon densities, i.e. the sets 2 and 3 [8], both of which describe the H1 data on the structure function

F_2. Note, Cascade simulates neither resolved photon processes nor MPI.

The mean charged particle multiplicities as a function of $P_{\mathrm{T,jet1}}$ in the *Toward* and *Away region* are shown in [1, 2] for direct and resolved enhanced events separately. The direct-dominated data are well described by both Pythia and Cascade. The resolved-dominated data are best described by Pythia with MPI. The contribution from MPI is largest at low $P_{\mathrm{T,jet1}}$. Cascade provides a reasonable description, except possibly at the lowest $P_{\mathrm{T,jet1}}$. The multiplicities as a function of $P_{\mathrm{T,jet1}}$ in the *High* and *Low activity regions* are shown in Fig.3. The direct-enhanced region ($x_\gamma > 0.7$) is again similarly well described by both Pythia with MPI and by Cascade. The resolved-enhanced region ($x_\gamma < 0.7$) is reasonably well described by Pythia with MPI. Cascade fails, but it is however closer to the data than Pythia without MPI.

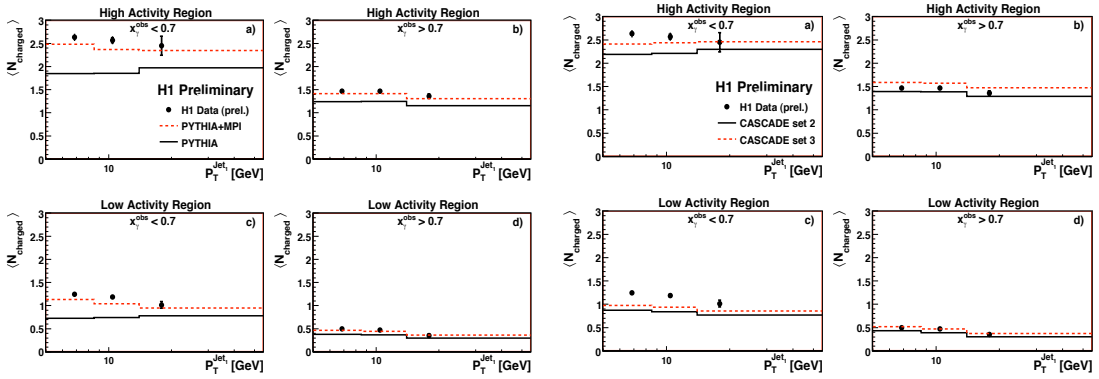

Figure 3: Mean charged particle multiplicity as a function of $P_{\mathrm{T,jet1}}$ in the *High* and *Low activity regions* for direct ($x_\gamma > 0.7$) and resolved ($x_\gamma < 0.7$) enhanced events. The data are compared to Pythia with and without MPI on the left and to Cascade for two different un-integrated gluon densities (sets 2 and 3) on the right.

It is interesting to note that Cascade is only somewhat worse in describing the resolved data, but is significantly better than Pythia without MPI. This is probably due to its different ansatz in calculating the primary hard interactions. If this picture could be confirmed, it would imply a smaller contribution from MPI. Clearly further studies at HERA and hadron-hadron colliders are needed.

3 High scales: Jet cross sections and $\alpha_s(M_Z)$ in DIS and PHP

In jet production in DIS there are two relevant high scales, i.e. Q and $P_{\mathrm{T,jet}}$, while in PHP there is only $P_{\mathrm{T,jet}}$. In order to have a smooth transition from DIS to PHP the scale $\sqrt{(Q^2 + P^2_{\mathrm{T,jet}})/2}$ is often used. In DIS we can have a more complicated interplay of the two scales. Depending on the kinematic regions in Q and $P_{\mathrm{T,jet}}$, either one of them can be larger than the other or they both can have rather similar magnitude. The precise measurements of jet cross sections in PHP and DIS by H1 and ZEUS are found to agree very well with NLO QCD calculations

such that precise values of the strong coupling $\alpha_s(M_Z)$ can be extracted.

A new preliminary extraction of $\alpha_s(M_Z)$ was obtained from a QCD re-analysis by ZEUS [10] of inclusive jet cross sections as a function of $E_{\mathrm{T,jet}}$ in PHP [9] from HERA-1. It is based on next-to-leading (NLO) pQCD calculations [12] and an estimation of the theoretical error from missing higher orders [11] not involving a refit of the data. This minimizes the theoretical error and leads to one of the most precise determinations of $\alpha_s(M_Z)$ at HERA. The method to extract α_s consisted of performing the NLO calculations with more recent PDFs [13], which had been extracted assuming different values of $\alpha_s(M_Z)$ when making the fits. The same value of $\alpha_s(M_Z)$ was used consistently in the calculation of the matrix elements and in the evolution of the PDFs. For the photon the GRV-HO [14] PDFs were used. The factorization and renormalization scales were set to $\mu_{\mathrm{R}} = \mu_{\mathrm{F}} = E_{\mathrm{T,jet}}$ of each jet.

The published data [9] and the new predictions are shown on the left of Fig. 4. The theoretical uncertainties indicated include those due to the conventional but arbitrary variation of the renormalization and factorization scales by a factor of 1/2 and 2, the PDF and the hadronization uncertainties. The dominant experimental error is due to the jet energy scale uncertainty of $\leq 1.5\,\%$. The extracted value for the strong coupling

$$\alpha_s(M_Z) = 0.1223 \pm 0.0001\,(\mathrm{stat})\,^{+0.0023}_{-0.0021}(\mathrm{exp})\ \pm 0.0030\,(\mathrm{theory})$$

is very similar to the older published one, but the theoretical uncertainty is reduced. The total uncertainty of $3.1\,\%$ is dominated by the theory uncertainty; the experimental contribution is $1.8\,\%$.

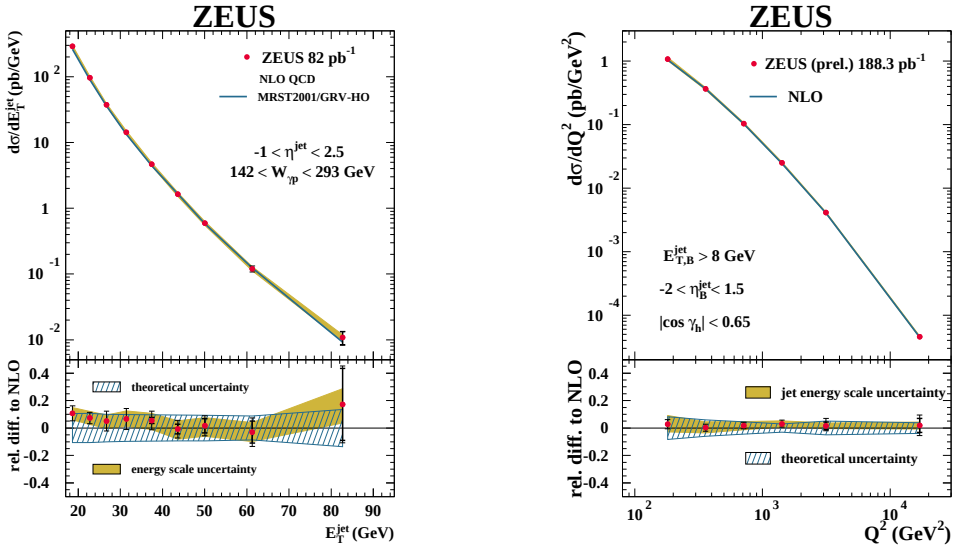

Figure 4: Inclusive jet cross section as a function of $E_{\mathrm{T,jet}}$ in PHP (left) and as a function of Q^2 in DIS (right) compared to NLO predictions.

New preliminary results from ZEUS [15] on single and double differential inclusive jet cross sections in neutral current DIS as a function of Q^2, $E_{\mathrm{T,jet}}$ and η_{jet} were presented this year. They made use of HERA-2 data corresponding to an integrated luminosity of 188 pb^{-1}. The

DIS phase space was defined by requiring $Q^2 > 125\,\mathrm{GeV}^2$ and the angle of the hadronic system $|\cos\gamma_h| < 0.65$. The jets were identified in the Breit frame [16] using the $k_\perp$ cluster algorithm [4]. In this frame they were required to have $E_{\mathrm{T,jet}} > 8$ GeV and $-2.0 < \eta_{\mathrm{jet}} < 1.5$. The dependence of the inclusive jet cross section on Q^2 is shown on the right of Fig. 4. The dominant experimental error is due to the jet energy scale uncertainty of $\leq 1.9\,\%$. The NLO predictions are shown to be in excellent agreement with the data. These calculations were performed using the program DISENT based on the dipole subtraction method [17]. The scales were chosen to be $\mu_{\mathrm{R}} = E_{\mathrm{T,jet}}$ and $\mu_{\mathrm{F}} = Q$, and for the proton PDFs the ZEUS-S parameterization [18] was taken. For the extraction of $\alpha_s(M_Z)$ the same method was used as described above for the jets in PHP. The theory uncertainty on $\alpha_s(M_Z)$ due to higher orders was estimated using the same method [11] as for the preliminary PHP result. The smallest error on $\alpha_s(M_Z)$ was obtained by fitting the Q^2 dependence for $Q^2 > 500\,\mathrm{GeV}^2$. In this region the experimental uncertainties are smaller than at lower Q^2, and also the theoretical uncertainties due to the PDFs and the missing higher orders are minimized, yielding:

$$\alpha_s(M_Z) = 0.1192 \pm 0.0009\,(\mathrm{stat})\,^{+0.0035}_{-0.0032}(\mathrm{exp})\,^{+0.0020}_{-0.0021}\,(\mathrm{theory})\,.$$

The total uncertainty is 3.5 %; in this case the experimental contribution of 2.9 % is somewhat larger than the theoretical one.

H1 has provided new single and double differential measurements of normalized NC jet cross sections [19], i.e. the ratio of inclusive jet, 2-jet and 3-jet cross sections to the inclusive DIS cross sections. By measuring normalized jet cross sections a number of experimental errors cancel partially, the luminosity error cancels completely, and the PDF uncertainty is also reduced. The dominant experimental error is due to the $\leq 1.5\,\%$ uncertainty on the jet energy scale. The data sample analyzed is from the years 1999 to 2007 and corresponds to an integrated luminosity of 395 pb^{-1}. The range covered in photon virtuality is $150 < Q^2 < 15000\,\mathrm{GeV}^2$ and in inelasticity $0.2 < y < 0.7$. The jet finding was performed in the Breit frame using the longitudinally invariant $k_\perp$ algorithm. Jets are accepted if in the laboratory frame they have $-0.8 < \eta_{\mathrm{jet}} < 2.0$. Furthermore, in the Breit frame the requirements are $P_{\mathrm{T,jet}} > 7$ GeV for inclusive jets and $P_{\mathrm{T,jet}} > 5$ GeV and additionally $M_{1,2} > 16$ GeV for 2-jet and 3-jet events. The normalized cross sections are measured as a function of Q^2, the jet transverse momentum and the proton momentum fraction [19].

Here, in Fig. 5, only the Q^2 dependence of the normalized inclusive jet and 2-jet cross section is shown. The NLO predictions for the jet cross sections were performed using the program NLOJET++ [20], and for the NC DIS cross sections the program DISENT [17] was used. The PDFs of the proton were taken from the CTEQ6.5M set [22]. For the jet calculations the factorization scale was taken to be $\mu_{\mathrm{F}} = Q$ and the renormalization scale to be $\mu_{\mathrm{R}} = \sqrt{(Q^2 + P_{\mathrm{T}}^2/2)/2}$, with P_{T} denoting the $P_{\mathrm{T,jet}}$ of the respective inclusive jet, or the arithmetic mean of the $P_{\mathrm{T,jet}}$ of the 2-jets or 3-jets. This choice is motivated by the presence of two hard scales in jet production in DIS. The theoretical errors on the normalized jet cross sections were determined in a similar way as described before for the ZEUS data.

For the extraction of the strong coupling, the jet cross sections were calculated as a function of $\alpha_s(\mu_{\mathrm{R}})$ using the FastNLO program [23], which allows to efficiently calculate cross sections based on the matrix elements from NLOJET++ and DISENT convoluted with the PDFS of the proton. From the measurements and predictions a $\chi^2(\alpha_s)$ was calculated using the Hessian method [24]. This method takes the correlations of experimental uncertainties into account. The dominant theory error is due to the uncertainty of the NLO prediction, which was estimated

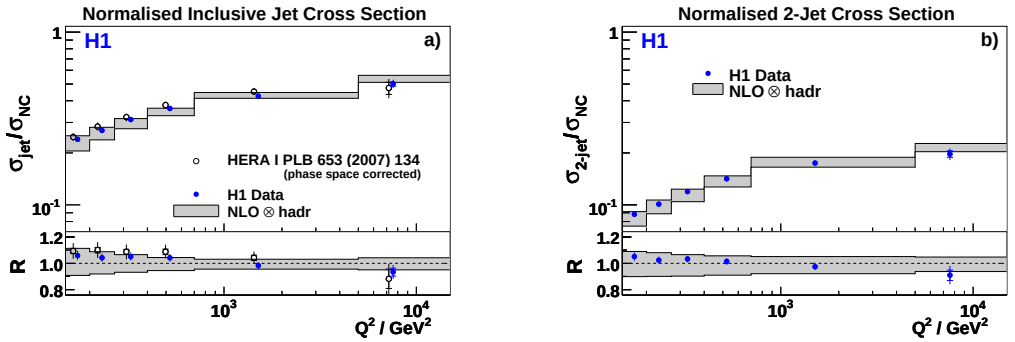

Figure 5: The normalized inclusive jet (left) and 2-jet (right) cross sections in NC DIS as functions of Q^2. They are compared to NLO predictions corrected for hadronization effects. The theory uncertainties associated with the renormalization and factorization scales, the PDFs and the hadronization are shown as grey bands.

by a variation of the renormalization and factorization scales by a factor of 1/2 and 2 of the nominal scale in fits of the data.

Fits of $\alpha_s(M_Z)$ to the individual normalized jet cross section data sets yielded consistent results. Therefore, all of them are used in a common fit taking correlations into account. This fit yields

$$\alpha_s(M_Z) = 0.1192 \pm 0.0007\,(\text{exp})\,^{+0.0046}_{-0.0030}\,(\text{theory})\;\pm 0.0016\,(\text{PDF})$$

with a fit quality $\chi^2/\text{ndf} = 65.0/53$. The total uncertainty of 3.6 % is dominated by the theory uncertainty; the experimental contribution is 0.6 % only.

On the left of Fig. 6 α_s is shown as a function of the scale Q extracted from the high Q^2 H1 data just discussed (6 rightmost points) and additionally as obtained from a preliminary low Q^2 H1 analysis [25]. The solid line shows the result of the evolution of the 2-loop solution of the renormalization group equation using the value of $\alpha_s(M_Z)$ extracted from the high Q^2 normalized jet cross sections. The inner (outer) band indicates the experimental (theoretical) uncertainties. As can be seen, the α_s values at low Q are nicely consistent with the prediction from high Q, and, interestingly, they lie within the theory uncertainty of the high Q^2 fit. When estimating the theory errors for the low Q values a much larger theoretical uncertainty is observed [25].

On the right of Fig. 6 the most recent values of $\alpha_s(M_Z)$ from jet measurements at HERA, from jet and event-shape measurements at LEP [27] and the 2009 world average by Bethke [27] are shown. The HERA $\alpha_s(M_Z)$ extractions have achieved an experimental precision compatible and competitive with the result from LEP and the world average. At this point in time the uncertainties at HERA are dominated by the NLO theory uncertainty. While advances in theory are most promising and most needed for being able to reduce the total uncertainty, one may also expect further experimental improvements by finalizing the analysis of all HERA data and by combining measurements from H1 and ZEUS.

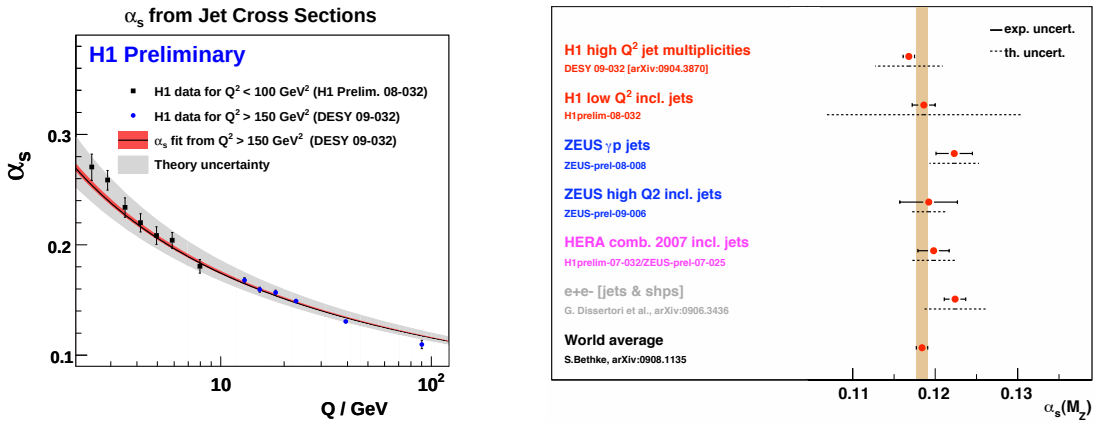

Figure 6: The running of the strong coupling as a function of the scale Q. The line shows the result of evolving the value of $\alpha_s(M_Z)$ extracted from the high Q^2 normalized jet cross sections down to the values of α_s obtained from the low Q^2 inclusive jet cross sections.

4 Multiple scales: Heavy flavor production

According to pQCD calculations, heavy quarks are mainly produced via the direct photon gluon fusion process $\gamma g \to Q\bar{Q}$. Therefore, measurements of $Q\bar{Q}$ production provide information on the gluon content of the proton. The heavy quark mass M is an additional hard scale in the calculations besides the momentum transfer of the exchanged photon Q and the transverse momentum P_{T} of the heavy quark. Due to this multi-scale problem, different approaches exist in the treatment of the pQCD series, depending on the relative magnitude of M, Q and P_{T}.

- At low scales when Q and $P_{\mathrm{T}} \approx M$, calculations in the *massive* fixed flavor number scheme (FFNS) appear appropriate. In this scheme the heavy quarks are produced only dynamically, they do not exist in the proton. The mass of the heavy quark is taken into account in the LO photon gluon fusion ($\gamma g \to Q\bar{Q}$) matrix element. NLO terms are of order α_s^2. Parton level calculations at NLO which take this approach are provided by the HVQDIS [29] program in DIS and by the FMNR [30] program in PHP. Also the PDF parameterizations CTEQ5F3 [31] and MRST2004FF3 [32] were obtained using this framework.

- At high scales when Q and $P_{\mathrm{T}} \gg M$, calculations in the zero mass variable flavor number scheme (ZM-VFNS) are applicable. In this scheme charm and beauty are treated as massless partons which exist already in the proton. At LO the quark parton model process ($\gamma Q \to Q$) provides the dominant contribution. At NLO photon gluon fusion and QCD Compton processes also contribute.

- Finally and more recently, calculations in the general mass variable flavor number scheme (GM-VFNS), which interpolate between the massless and the massive schemes, provide a description of heavy quark production over the whole range in Q^2. Such calculations are used in the latest global PDF fits, yielding the following PDF parameterizations: CTEQ6.6 NLO [33], MSTW08 NLO [34] and MSTW08 NNLO [34].

Measurements of the contributions of charm and beauty, $F_2^{c\bar{c}}$ and $F_2^{b\bar{b}}$, to the proton structure function F_2 allow to test these schemes. The gluon and heavy quark PDFs are important for the understanding of measurements of standard and beyond standard model physics processes at the TEVATRON and LHC. For this reason the focus here is on most recent measurements of charm and particularly beauty in DIS at HERA. Some of the results presented make use of the full HERA-2 data sample and thus offer a significant improvement in precision compared to previous HERA-1 results.

The fraction of charm production in total NC DIS is large, up to $\approx 30\%$ at HERA energies. Charm quarks are tagged predominantly by reconstructing the decays of charmed hadrons, $D^{\star\pm}$, $D^{\pm}$, $D_s^{\pm}$ and D^0 (see for example [35, 36]). The signal to background ratio of these measurements can be further improved by using information on the decay length provided by the decay vertex as reconstructed by the silicon vertex detectors of the H1 and ZEUS experiments.

Beauty quarks, in contrast to the large contribution of charm to deep-inelastic scattering, contribute at most a few % and an order of magnitude less at low Q^2. This makes the tagging of beauty in DIS events very challenging. To extract signals use is made of various properties of beauty hadrons: their semi-leptonic decays and their relatively large mass and long life-time. In semi-leptonic decays the large transverse momentum of the lepton w.r.t. the jet axis, $p_{\mathrm{T}}^{\mathrm{rel}}$, and the missing neutrino momentum projected onto the direction of the lepton, $p_{\mathrm{T}}^{\mathrm{miss}\|\mu}$, are used. In addition, information on the impact parameter δ of the lepton as obtained from the vertex detectors can be used. In analyses not requiring a lepton the impact parameter significance of all tracks with hits in the vertex detector and the distance significance of the secondary vertex are used by a neural network to discriminate between beauty, charm and light quarks. The c, b and light quark fractions in the data are extracted performing fits of simulated Monte Carlo (MC) templates to the measured distributions.

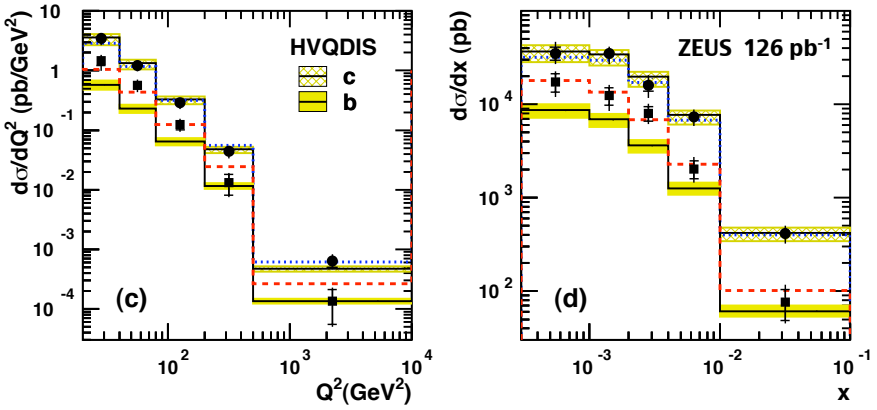

Figure 7: Differential muon cross sections for c and b production as a function of Q^2 and x. The bands show the NLO predictions by HVQDIS and the corresponding uncertainties.

Inclusive charm and beauty cross sections were measured by ZEUS [37] based on 126 pb^{-1} of HERA-2 data, using semi-leptonic decays of heavy hadrons into muons. The kinematic phase space covered is given by $Q^2 > 20\,\mathrm{GeV}^2$, the inelasticity $0.01 < y < 0.7$, $P_{\mathrm{T}}{}^{\mu} > 1.5$ GeV and $-1.6 < \eta^{\mu} < 2.3$. The charm and beauty contributions were extracted by simultaneous

fits of MC templates to the muon $p_{\mathrm{T}}^{\mathrm{rel}}$, $p_{\mathrm{T}}^{\mathrm{miss}\|\mu}$ and δ distributions (see [1, 37]). The relatively low cut on $P_{\mathrm{T}}{}^{\mu}$ allows both, the inclusive charm and beauty cross sections to be determined simultaneously as a function of $P_{\mathrm{T}}{}^{\mu}$, η^{μ}, Q^2 and x. They are shown as a function of Q^2 and x in Fig. 7 (see [1, 37] for the dependence on $P_{\mathrm{T}}{}^{\mu}$ and η^{μ}). The charm data are well described by HVQDIS, while for beauty the data lie above the predictions at low Q^2 and x. The measurements were extrapolated to the full phase space to provide charm and beauty structure functions (see Fig. 8 and Fig. 9 to be discussed below).

The H1 collaboration provided new data on the inclusive production of charm and beauty in DIS [38] in the kinematic region $5 < Q^2 < 650\,\mathrm{GeV}^2$ and $0.0002 < x < 0.032$ corresponding to an integrated luminosity of 189 pb^{-1}. This analysis used the impact parameter significance of tracks and the distance significance from the primary vertex to the decay vertex of the heavy hadrons as inputs to a neural network (see [1, 38]. As in the ZEUS analysis the charm and beauty contributions were obtained from fits of various distributions to MC templates. From these the visible cross sections were determined and extrapolated to the full phase space, providing measurements of the charm and beauty structure functions $F_2^{c\bar{c}}$ and $F_2^{b\bar{b}}$ respectively.

The results for $F_2^{b\bar{b}}$ together with the ones from ZEUS discussed above are shown in Fig. 8 as a function of Q^2 for different fixed values of x. They are in reasonable agreement, although the ZEUS results tend to be higher than the ones from H1 at low Q^2. The measurements of $F_2^{b\bar{b}}$ are well described by the latest GM-VFNS calculations (MSTW08) in NLO and NNLO. In the phase space region of the measurements the differences between NLO and NNLO are tiny, except for $Q^2 < M_b^2$.

A large number of measurements of the charm structure function $F_2^{c\bar{c}}$ using different methods are shown in Fig. 9 as a function of Q^2 for various fixed values of x. The data cover a large phase space in Q^2 and x due to the substantially higher statistics for charm. The acceptance of the different methods varies between 20% and 70%, but the results

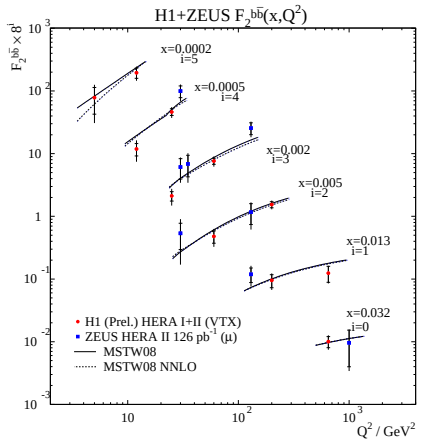

Figure 8: The structure function $F_2^{b\bar{b}}$ as a function of Q^2 for fixed values of x. Also shown are the GM-VFNS predictions MSTW08 in NLO and NNLO.

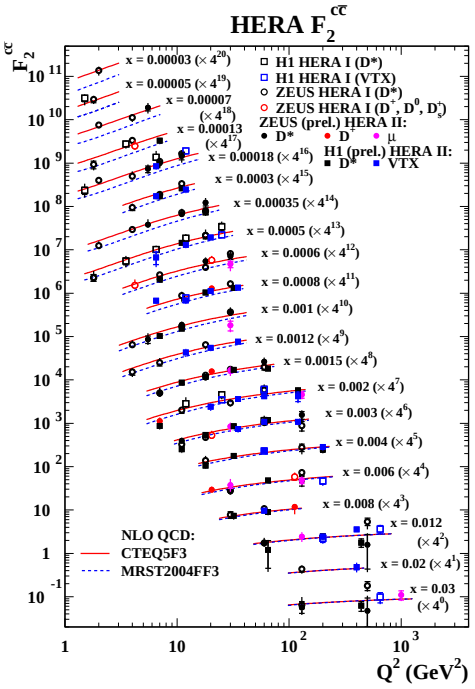

Figure 9: The structure function $F_2^{c\bar{c}}$ as a function of Q^2 for fixed values of x. Also shown are the massive FFNS predictions CTEQ5F3 and MRST2004FF3 in NLO.

agree well between them. The theory prediction based on the massive FFNS provides a reasonable description of the data. The largest differences between the CTEQ5F3 and MRST2004FF are in the region $Q^2 < 2M_c^2$ due to different inputs in this region when fitting the PDFs. The precision in $F_2^{c\bar{c}}$ and $F_2^{b\bar{b}}$ can be expected to be further improved by analyzing the full HERA statistics and by combining results using different methods within an experiment and within H1 and ZEUS.

5 Summary

Low & high scales – The study of the underlying event, which involves an understanding of the physics at high and at low scales, indicates that in resolved photon interactions the description of the mean charged particle multiplicity in different azimuthal regions requires multiple interactions when using Pythia to describe the data. The comparison of the data with CASCADE, which provides a different approach to hard interactions and also includes no MPI, suggests that within this model the importance of the underlying event is reduced. This requires further studies. If correct, this of course would have interesting and important consequences, particularly for understanding the data at the TEVATRON and LHC.

High scales – Jet production in DIS and PHP are found to be well described by NLO QCD. This allows for precise extractions of the strong coupling $\alpha_s(M_Z)$, competitive and compatible with results from e^+e^- annihilation at LEP and the world average. The experimental precision reached so far is among the best of the various measurements, however the theoretical precision at NLO is considerably worse. A significant increase in total precision can be expected from the calculation of higher orders beyond NLO.

Multiple high scales – The physics of charm and beauty production at HERA involves the interplay of the hard scales M, Q and P_{T}. Experimentally, many different techniques to tag charm or beauty have been employed for the measurement of differential cross sections and their extrapolation to the total inclusive cross sections or structure functions $F_2^{c\bar{c}}$ and $F_2^{b\bar{b}}$. They are all found to be overall well described by QCD calculations.

Work is continuing at HERA towards final results by analyzing the complete HERA data set with improved understanding of the detector and event reconstruction, and by combining H1 and ZEUS measurements.

6 Acknowledgments

I want to thank my colleagues in H1 and ZEUS who provided suggestions and help in preparing this talk. Thanks also to the organizers for this interesting conference.

7 Bibliography

References

[1] Slides: `http://indico.desy.de/contributionDisplay.py?contribId=27&sessionId=9&confId=1407`

[2] H1 Collaboration, *"Study of Multiple Interactions in Photoproduction at HERA"*, H1prelim-08-036.

[3] T. Affolder *et al.* [CDF Collaboration], Phys. Rev. D **65** (2002) 092002.

[4] S. Catani, Y.L. Dokshitzer, M.H. Seymour and B.R. Webber, Nucl. Phys. B **406** (1993) 187.

[5] T. Sjöstrand, S. Mrenna and P. Skands, JHEP **0605** (2006) 026 [arXiv:hep-ph/0603175].

[6] H. Jung and G.P. Salam, Eur. Phys. J. C **19** (2001) 351 [arXiv:hep-ph/0012143].

[7] H. Jung, Comput. Phys. Commun. **143** (2002) 100 [arXiv:hep-ph/0109102].

[8] M. Hansson and H. Jung, "Status of CCFM: Un-integrated gluon densities," arXiv:hep-ph/0309009.

[9] S. Chekanov *et al.* [ZEUS Collaboration], Phys. Lett. B **560** (2003) 7 [arXiv:hep-ex/0212064].

[10] ZEUS Collaboration, *"α_s from inclusive-jet cross sections in photoproduction at ZEUS"*, ZEUS-prel-08-008.

[11] R.W.L. Jones, M. Ford, G.P. Salam, H. Stenzel and D. Wicke, JHEP **0312** (2003) 007 [arXiv:hep-ph/0312016].

[12] M. Klasen, T. Kleinwort and G. Kramer, Eur. Phys. J. direct C **1** (1998) 1 [arXiv:hep-ph/9712256].

[13] A.D. Martin, R.G. Roberts, W.J. Stirling and R.S. Thorne, Eur. Phys. J. C **23** (2002) 73 [arXiv:hep-ph/0110215].

[14] M. Gluck, E. Reya and A. Vogt, Phys. Rev. D **45** (1992) 3986.

[15] ZEUS Collaboration, *"Inclusive-jet production in NC DIS with HERA II"*, ZEUS-prel-09-006.

[16] R.P. Feynman, "*Photon-Hadron Interactions.*" Benjamin, New York, (1972); K.H. Streng, T.F. Walsh and P.M. Zerwas, Z. Phys. C **2** (1979) 237.

[17] S. Catani and M.H. Seymour, Nucl. Phys. B **485** (1997) 291 [Erratum-ibid. B **510** (1998) 503] [arXiv:hep-ph/9605323].

[18] S. Chekanov *et al.* [ZEUS Collaboration], Phys. Rev. D **67** (2003) 012007 [arXiv:hep-ex/0208023].

[19] F.D. Aaron *et al.* [H1 Collaboration], arXiv:0904.3870 [hep-ex], to be published in Eur. Phys. J. C.

[20] Z. Nagy and Z. Trocsanyi, Phys. Rev. Lett. **87** (2001) 082001 [arXiv:hep-ph/0104315].

[21] J. Pumplin, D.R. Stump, J. Huston, H.L. Lai, P.M. Nadolsky and W.K. Tung, JHEP **0207** (2002) 012 [arXiv:hep-ph/0201195].

[22] W.K. Tung, H.L. Lai, A. Belyaev, J. Pumplin, D. Stump and C.P. Yuan, JHEP **0702** (2007) 053 [arXiv:hep-ph/0611254].

[23] T. Kluge, K. Rabbertz and M. Wobisch, published in procs. of "Deep-Inelastic Scattering DIS 2006", eds. M. Kuze *et al.*, 483, arXiv:hep-ph/0609285.

[24] M. Botje, Eur. Phys. J. C **14** (2000) 285 [arXiv:hep-ph/9912439].

[25] H1 Collaboration, *"Inclusive Jet Production at low Q^2 and determination of α_s"*, H1prelim-08-032.

[26] S. Kluth, J. Phys. Conf. Ser. **110** (2008) 022023 [arXiv:0709.0173 [hep-ex]].

[27] S. Bethke, "The 2009 Wolrd Average of $\alpha_s(M_Z)$," arXiv:0908.1135 [hep-ph].

[28] J. Smith and W.L. van Neerven, Nucl. Phys. B **374** (1992) 36.

[29] B.W. Harris and J. Smith, Phys. Rev. D **57** (1998) 2806 [arXiv:hep-ph/9706334].

[30] S. Frixione, M.L. Mangano, P. Nason and G. Ridolfi, Nucl. Phys. B **412** (1994) 225 [arXiv:hep-ph/9306337].

[31] H. L. Lai *et al.* [CTEQ Collaboration], Eur. Phys. J. C **12** (2000) 375 [arXiv:hep-ph/9903282].

[32] A. D. Martin, W. J. Stirling and R. S. Thorne, Phys. Lett. B **636** (2006) 259 [arXiv:hep-ph/0603143].

[33] P. M. Nadolsky *et al.*, Phys. Rev. D **78** (2008) 013004 [arXiv:0802.0007 [hep-ph]].

[34] A.D. Martin, W.J. Stirling, R.S. Thorne and G. Watt, arXiv:0901.0002 [hep-ph].

[35] H1 Collaboration, *"$D^\star$ production at low Q^2 with the H1 detector"*, H1prelim-08-072; *"$D^\star$ production at high Q^2 with the H1 detector"*, H1prelim-08-074.

[36] S. Chekanov *et al.* [ZEUS Collaboration], arXiv:0812.3775 [hep-ex].

[37] S. Chekanov *et al.* [ZEUS Collaboration], arXiv:0904.3487 [hep-ex].

[38] F.D. Aaron *et al.* [H1 Collaboration], arXiv:0907.2643 [hep-ex].